

MAKING MEDICAL VISION-LANGUAGE MODELS THINK CAUSALLY

ACROSS MODALITIES WITH RETRIEVAL-AUGMENTED CROSS-MODAL REASONING

Weiqin Yang^{1,*} Haowen Xue^{2,*,†} Qingyi Peng³ Hexuan Hu² Qian Huang² Tingbo Zhang²¹University of Adelaide ²Hohai University ³Amap

ABSTRACT

Medical vision–language models (VLMs) achieve strong performance in diagnostic reporting and image–text alignment, yet their underlying reasoning mechanisms remain fundamentally correlational, exhibiting reliance on superficial statistical associations that fail to capture the causal pathophysiological mechanisms central to clinical decision-making. This limitation makes them fragile, prone to hallucinations, and sensitive to dataset biases. Retrieval-augmented generation (RAG) offers a partial remedy by grounding predictions in external knowledge. However, conventional RAG depends on semantic similarity, introducing new spurious correlations. We propose Multimodal Causal Retrieval-Augmented Generation (MCRAG), a framework that integrates causal inference principles with multimodal retrieval. MCRAG retrieves clinically relevant exemplars and causal graphs from external sources, conditioning model reasoning on counterfactual and interventional evidence rather than correlations alone. Applied to radiology report generation, diagnosis prediction, and visual question answering, MCRAG improves factual accuracy, robustness to distribution shifts, and interpretability. Our results highlight causal retrieval as a scalable path toward medical VLMs that think beyond pattern matching, enabling trustworthy multimodal reasoning in high-stakes clinical settings.

Index Terms— Vision–Language Models, Retrieval-based Inference, Causal Inference, Multimodal Reasoning

1. INTRODUCTION

Artificial Intelligence (AI) has already transformed healthcare and continues to hold substantial potential for further innovation within clinical ecosystems. Recently, Medical Large Vision-Language Models (Med-LVLMs) have shown great promise for advancing interactive and intelligent diagnosis [1, 2]. Despite this potential, current Med-LVLMs still face significant reliability issues, particularly their tendency to generate non-factual medical responses [3], making them unreliable in critical medical applications. These factuality issues raise serious concerns when deploying such models in clinical

settings, where even small diagnostic errors could lead to severe consequences for patient care.

Recently, researchers have begun to focus on improving the factuality of Med-LVLMs through various techniques, including fine-tuning [1], low-rank adaptation [4], and retrieval-augmented generation (RAG) [5, 6]. Fine-tuning is a direct method to improve model performance, but faces several limitations in the medical field. First, there is a lack of sufficient high-quality labeled data for fine-tuning in the medical domain. Second, a distribution shift often exists between training datasets and the real-world deployment data, leading to significantly worse model performance during deployment. Hence, Retrieval-Augmented Generation (RAG) [5] has emerged as a promising solution, grounding model outputs in external knowledge to improve factuality. Recent works adapted RAG for medicine, including MedRAG [6], MMed-RAG [7]. Despite improvements, current methods remain vulnerable to semantic over-reliance, cross-modality misalignment, and spurious correlations, largely due to mismatch between retrieved contexts and visual–language grounding.

Causality-based methods seek to improve retrieval accuracy and representation learning, but critical limitations persist [8]. CausalRAG [9] ranks contexts by causal importance, but does not address cross-modal alignment. Similarly, CM-CRL [10] learns shared causal representations but underuses the structural dependencies needed for medical reasoning. Although causal graphs improve interpretability [11, 12], current approaches mainly rely on language-only causal discovery [9].

These limitations necessitate a more holistic framework that simultaneously addresses factuality and alignment by integrating causal reasoning with a multimodal structure. Accordingly, we propose to build explicit causal graphs from multimodal data and use them to guide RAG retrieval for medical reasoning.

In this paper, we propose MCRAG (Multimodal Causal Retrieval-Augmented Generation), a retrieval framework designed to improve factuality and robustness in Med-LVLMs. MCRAG introduces a causal alignment graph constructed from verifiable medical literature, capturing structured dependencies between visual and textual modalities. This graph enables retrieval guided not only by semantic similarity but also by causal and structural relevance, thus mitigating spuri-

* Equal contribution. † Corresponding author.

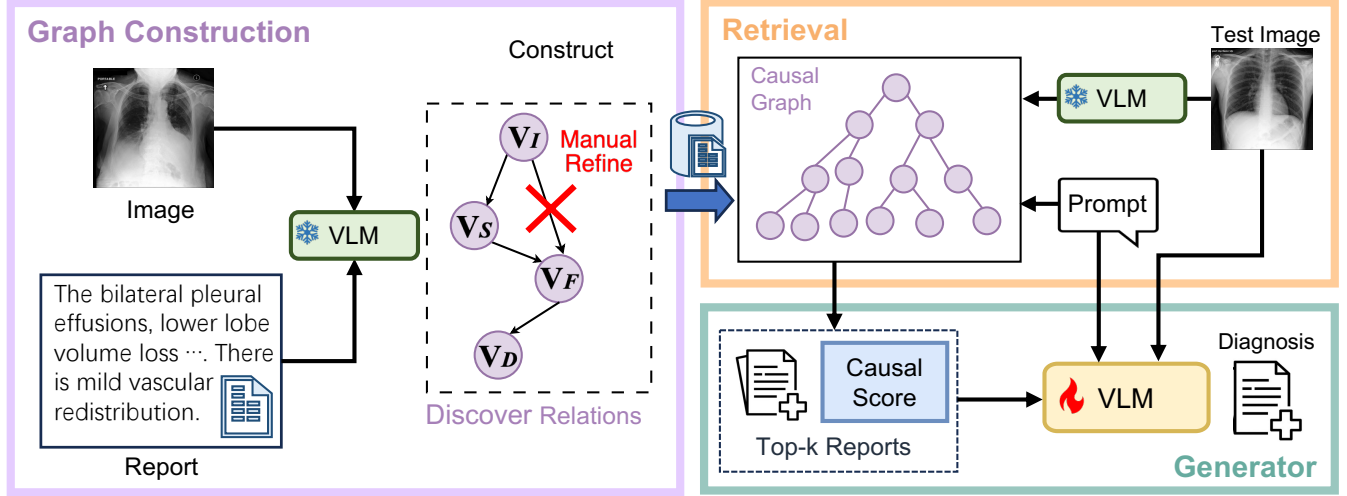


Fig. 1: MCRAG overview. Left (Graph Construction): A VLM extracts entities and relations from paired images and reports to construct a causal graph, followed by manual refinement to prune spurious links. Right (Retrieval and Generation): For a test image, the VLM queries the causal graph to retrieve top-k relevant reports ranked by a causal score. The retrieved reports and test image are then combined into a prompt for the generator VLM, which produces the final diagnosis.

ous correlations. Furthermore, MCRAG incorporates RAG-based preference fine-tuning to enforce two key principles: (i) grounding responses in input images when relevant to prevent degenerate text-only outputs; and (ii) interpreting retrieved contexts causally to enhance robustness under uncertainty. Finally, MCRAG applies causal filtering to balance coverage and precision in retrieval, selecting context based on structural importance rather than raw similarity.

Our contributions are threefold.

- **MCRAG:** We introduce the first framework that integrates causal graphs with cross-modal alignment for medical vision–language generation.
- **Causal alignment graph:** We design a knowledge-guided graph that enables structured cross-modal retrieval grounded in medical semantics.
- **Preference fine-tuning:** We propose a strategy that enforces image-grounded, causally coherent generation, improving robustness and factual accuracy across medical tasks.

2. METHODOLOGY

In this section, we present **MCRAG**—a multi-modal, causal retrieval-augmented generation framework that improves the factuality of Med-LVLMs by tightly coupling retrieval with an explicit Structural Causal Model (SCM). The framework has three stages: (1) *domain-aware retrieval*, which selects the optimal retriever for each input; (2) *adaptive context selection*, which filters and sizes evidence on the fly; and (3)

RAG-based preference fine-tuning, which aligns responses with SCM-supported evidence.

2.1. Structural Causal Model (SCM)

At the core of the MCRAG framework is the formal representation of medical knowledge as a *Structural Causal Model* (SCM), a mathematical formalism for causal inference. An SCM, denoted as \mathcal{M} , is a tuple $\langle \mathbf{V}, \mathbf{U}, \mathcal{F} \rangle$, where:

- \mathbf{V} is a set of endogenous variables, representing the manifest, observable variables within the system. In the medical context, \mathbf{V} includes variables corresponding to image regions (V_I), clinical findings (V_F), patient symptoms (V_S), and diagnostic outcomes (V_D).
- \mathbf{U} is a set of exogenous variables, representing latent or unobserved factors. These variables account for all factors influencing the endogenous variables that are not explicitly included in the model, such as genetic predispositions or data heterogeneity across hospital systems.
- \mathcal{F} is a set of structural equations, one for each variable $V_i \in \mathbf{V}$. Each equation $f_i \in \mathcal{F}$ defines the value of V_i as a function of its parents, $\text{Pa}(V_i)$, in the causal graph and its corresponding exogenous variable $U_i \in \mathbf{U}$. For instance, a function for a specific clinical finding might be expressed as:

$$\hat{V}_F = f_F(\text{Pa}(V_F), U_F) \quad (1)$$

A key feature of the SCM is its associated causal graph G , a directed graph over the variables in \mathbf{V} and \mathbf{U} .

2.2. Cross-Modal Medical Causal Graph Construction

The construction of a comprehensive causal graph G requires integrating information from multiple modalities. Our framework employs a two-stage data-driven causal discovery protocol to build G from a corpus of paired medical images and clinical reports.

Step 1: Multimodal VLMs-Assisted Causal Discovery

We use vision-Language Models (VLMs) to serve as the primary knowledge extractor. The model is prompted to analyze image-text pairs to identify potential causal relationships. For instance, a visual feature like ‘**pulmonary opacity**’ observed in a chest X-ray would be linked to the textual entity ‘**pneumonia**’ in the accompanying report, proposing a causal edge between them, grounding textual concepts in visual evidence. Let v_i and r_j denote the visual embedding of image i and textual report embedding of report j , respectively. The retriever’s contrastive loss $\mathcal{L}_{\text{retr}}$ maximizes the cosine similarity $s_{ij} = \langle v_i, r_j \rangle$ for true image-report pairs while minimizing s_{ij} for mismatched pairs. In practice, we collect a corpus of domain-specific text (e.g. reports for radiology images) and use these as the knowledge base.

Step 2: Manual Graph Refinement. Starting from the draft graph proposed by the VLMs under a low-confidence threshold, we conduct a principled manual review of every candidate causal edge. Each edge is evaluated for clinical plausibility and statistical support (e.g., whether the conditional probability of a diagnosis given a visual feature corresponds with domain knowledge), and any edge failing this inspection is removed. For instance, if a visual feature V_I and the final diagnosis V_D are conditionally independent given a textual clinical finding V_F (i.e., $V_I \perp\!\!\!\perp V_D \mid V_F$), this provides statistical evidence for the causal pathway $V_I \rightarrow V_F \rightarrow V_D$ and justifies pruning the spurious direct edge $V_I \rightarrow V_D$. Clinically unreasonable edges are discarded even if strong statistical associations appear.

2.3. Causal-based Retrieval Augmented Reasoning

Given an input image I , we first retrieve the top- K nearest textual reports $\{R_k\}_{k=1}^K$ in a joint embedding space. We then enforce causal consistency using the graph G . For each candidate R_k , we extract the variables it references (e.g., findings V_F and diagnoses V_D) and evaluate how well they are supported by image-derived features V_I along the causal paths in G (preferably $V_I \rightarrow V_F \rightarrow V_D$).

$$\begin{aligned} \text{Score}(R_k) = & (1 - \alpha) \log p_G(V_D, V_F \mid V_I) \\ & + \alpha \text{sim}(I, R_k), \quad \alpha \in [0, 1] \end{aligned} \quad (2)$$

where $\text{sim}(I, R_k)$ denotes the image-report embedding similarity, and $p_G(\cdot)$ is the likelihood induced by the factorization

implied by the causal graph G . For example, if G retains the mediated path $V_I \rightarrow V_F \rightarrow V_D$, then

$$p_G(V_D, V_F \mid V_I) = p(V_F \mid V_I) p(V_D \mid V_F) \quad (3)$$

Candidates consistent with G are up-weighted, whereas those relying on unsupported or pruned edges are down-weighted or discarded, yielding retrieved reports that are both semantically relevant and causally grounded.

After assembling high-quality retrieved contexts and their associated causal relations, MCRAG integrates them into the generation process via retrieval-augmented fine-tuning.

3. EXPERIMENT

3.1. Experimental Setups

For the language model, we adopt LLaVA-Med-1.5-7B [1], fine-tuned with LoRA [19] using the AdamW optimizer. The fine-tuning is performed with a learning rate of 3×10^{-5} , weight decay of 10^{-2} , a batch size of 16, and for 500 epochs. For modality-specific encoders, we employ MedViT [20] as the vision encoder and BioClinicalBERT [21] as the text encoder.

We adopt the experimental framework of MMed-RAG[7] and evaluate hallucination mitigation methods from two complementary perspectives. Decoding-based approaches, such as DoLa [13], OPERA [14], and VCD [15], improve factual consistency by directly adjusting the model’s output distribution. In contrast, multimodal retrieval-augmented generation (RAG) methods, including MedDr [16], FactMM-RAG [17], RULE [18], and MMed-RAG [7], mitigate hallucinations by grounding responses in external knowledge. We didn’t choose the CasualRAG is because it is not multi-modal, so not in our scope.

Our experiments employ MIMIC-CXR [22] and IU-Xray [23] as benchmark datasets. Question-answer pairs are taken from MMed-RAG [7]. Following prior work [7], we assess medical VQA performance using Accuracy, F1 Score, and AUROC, while report generation is evaluated with BLEU, ROUGE-L, and METEOR.

3.2. Comparison Results

Table 1 compares decoding-only baselines with retrieval-augmented models. While MMed-RAG delivers strong results (e.g., 89.54 Acc and 87.13 AUC on IU-Xray VQA), our method (MCRAG) consistently sets new state-of-the-art across all tasks. On IU-Xray VQA, MCRAG surpasses MMed-RAG by +0.58 Acc, +1.31 F1, and +1.12 AUC; on MIMIC-CXR VQA, it achieves further gains of +1.34 Acc, +0.88 F1, and +1.34 AUC. For report generation, MCRAG raises BLEU to 35.02 and 25.81, improving over MMed-RAG by +3.64 and +2.56 on IU-Xray and MIMIC-CXR, respectively. These results demonstrate that causality-guided retrieval not only enhances factual accuracy in VQA

Table 1: Performance (%) of different methods on Radiology VQA and Radiology Report Generation. For VQA, we report Accuracy, F1 score, and AUROC; for Report Generation, we report BLEU, ROUGE-L (R-L), and METEOR (MET). The best and second-best results are highlighted in red and blue, respectively. Comparison results are reported from MMed-RAG [7].

Models	Radiology VQA						Radiology Report Generation					
	IU-Xray			MIMIC-CXR			IU-Xray			MIMIC-CXR		
	Acc \uparrow	F1 \uparrow	AUC \uparrow	Acc \uparrow	F1 \uparrow	AUC \uparrow	BLEU \uparrow	R-L \uparrow	MET \uparrow	BLEU \uparrow	R-L \uparrow	MET \uparrow
LLaVA-Med-1.5 [1]	75.47	64.04	67.46	75.79	80.49	68.84	9.64	12.26	8.21	12.11	13.05	11.16
+ DoLa [13]	78.00	66.75	72.19	81.35	85.73	72.73	11.79	15.82	12.72	17.11	14.89	14.81
+ OPERA [14]	70.59	61.54	63.22	69.34	76.66	62.46	10.66	14.70	12.01	15.40	12.52	13.72
+ VCD [15]	68.99	54.35	61.08	70.89	75.57	64.61	10.42	14.14	11.59	15.18	12.30	13.38
+ MedDr [16]	83.33	67.80	77.15	55.16	56.18	58.47	12.37	16.45	13.50	18.59	15.72	16.77
+ FactMM-RAG [17]	84.51	68.51	77.07	77.58	81.86	70.09	14.70	18.05	15.92	18.71	15.84	16.82
+ RULE [18]	87.84	78.00	85.78	83.92	87.49	83.44	27.53	23.16	27.99	18.61	15.96	17.42
+ MMed-RAG [7]	89.54	80.72	87.13	83.57	88.49	85.08	31.38	25.59	32.43	23.25	12.34	20.47
+ MCRAAG	90.12	82.03	88.25	84.91	89.37	86.42	35.02	28.47	35.18	25.81	15.05	22.34

Table 2: Ablation study of causality in MCRAAG on the MIMIC-CXR dataset. We report Accuracy (Acc), F1, and BLEU as mean \pm std over 3 runs. τ denotes the ratio of causal branches removed for refining causal links.

Method	Acc \uparrow	F1 \uparrow	BLEU \uparrow
MCRAAG(Full Model, $\tau = 0.7$)	84.91 \pm 0.21	89.37 \pm 0.18	25.81 \pm 0.42
w/o Causality Relation	81.26 \pm 0.33	86.71 \pm 0.29	23.58 \pm 0.55
w/o Manual Refining	80.34 \pm 0.27	85.42 \pm 0.31	22.47 \pm 0.61
$\tau = 0.5$	83.47 \pm 0.24	87.92 \pm 0.22	24.71 \pm 0.48
$\tau = 0.7$ (ours)	84.91 \pm 0.21	89.37 \pm 0.18	25.81 \pm 0.42
$\tau = 0.9$	84.12 \pm 0.26	88.41 \pm 0.25	25.02 \pm 0.47

but also yields more fluent, faithful clinical reports.

Ablation Studies. To understand the role of causality, we ablate both its presence and the ratio used for refining (i.e., the percentage of the causal branch manually removed). As shown in Table 2, removing causality causes the steepest drop (-3.65 Acc, -3.95 F1, -3.34 BLEU), highlighting its central role in grounding answers in clinically meaningful evidence. Using causality without refining partially recovers performance but still introduces noisy links. Introducing confidence-based refining steadily improves results, with the best trade-off observed at $\tau = 0.7$ (84.91 Acc, 89.37 F1, 25.81 BLEU). Lower ratio (e.g., $\tau = 0.5$) allow noise to persist, while higher ratio (e.g., $\tau = 0.9$) over-prune and reduce recall. Causality thus drives robust reasoning by structuring the search space, while manually refining calibrates the precision–coverage trade-off by pruning unreliable links.

Table 3 shows that both re-ranking and filtering are crucial for RAG. Removing re-ranking reduces performance (83.78 Acc, 87.20 F1, 24.61 BLEU), while removing filtering leads to an even larger drop (82.15 / 85.40 / 23.20), indicating its stronger role. Varying K reveals the evidence–noise trade-off: too few reports ($K = 5$) limit coverage, too many ($K = 20$) add noise, and the best balance is at $K = 10$.

Table 3: Analysis of report usage in RAG with different retrieval settings. We report performance (mean \pm std over 3 runs). *Re-ranking* reorders retrieved reports, and *Filtering* removes low-quality ones by score threshold.

Method	Acc \uparrow	F1 \uparrow	BLEU \uparrow
RAG (Full Model, $K = 10$)	84.91 \pm 0.22	89.37 \pm 0.20	25.81 \pm 0.45
w/o Re-ranking	83.78 \pm 0.31	87.20 \pm 0.27	24.61 \pm 0.52
w/o Filtering	82.15 \pm 0.29	85.40 \pm 0.33	23.20 \pm 0.58
$K = 5$	84.10 \pm 0.25	87.40 \pm 0.28	25.00 \pm 0.49
$K = 10$ (ours)	84.91 \pm 0.22	89.37 \pm 0.20	25.81 \pm 0.45
$K = 20$	84.60 \pm 0.27	88.00 \pm 0.26	25.60 \pm 0.50

4. LIMITATIONS

While MCRAAG advances retrieval by incorporating causal reasoning, several limitations remain. The framework presupposes that VLM can reliably encode and expose causal structures; however, this assumption may not hold in domains characterized by highly specialized or rapidly evolving knowledge. Moreover, the identification of causal pathways during inference necessitates additional model queries, thereby increasing computational overhead and potentially constraining scalability in practical deployments.

5. CONCLUSION

We present MCRAAG, a multimodal causal retrieval framework that enhances factuality and robustness in medical vision–language models. By integrating graph-based causal reasoning within cross-modal retrieval, MCRAAG achieves state-of-the-art results on radiology-specific VQA and report generation tasks. Ablation analysis further underscores the importance of causal grounding for clinically meaningful evidence and demonstrates the effectiveness of manual refinement in improving precision. Taken together, these findings highlight causal retrieval as a viable pathway toward safer deployment in real-world clinical settings.

6. REFERENCES

[1] Chunyuan Li, Cliff Wong, Sheng Zhang, Naoto Usuyama, Haotian Liu, Jianwei Yang, Tristan Naumann, Hoifung Poon, and Jianfeng Gao, “Llava-med: Training a large language-and-vision assistant for biomedicine in one day,” *Advances in Neural Information Processing Systems*, vol. 36, pp. 28541–28564, 2023.

[2] Chaoyi Wu, Xiaoman Zhang, Ya Zhang, Yanfeng Wang, and Weidi Xie, “Towards generalist foundation model for radiology by leveraging web-scale 2d&3d medical data,” *arXiv preprint arXiv:2308.02463*, 2023.

[3] Jiawei Chen, Dingkang Yang, Tong Wu, Yue Jiang, Xiaolu Hou, Mingcheng Li, Shunli Wang, Dongling Xiao, Ke Li, and Lihua Zhang, “Detecting and evaluating medical hallucinations in large vision language models,” *arXiv preprint arXiv:2406.10185*, 2024.

[4] Edward J Hu, Yelong Shen, Phillip Wallis, Zeyuan Allen-Zhu, Yuanzhi Li, Shean Wang, Lu Wang, Weizhu Chen, et al., “Lora: Low-rank adaptation of large language models.,” *ICLR*, vol. 1, no. 2, pp. 3, 2022.

[5] Yunfan Gao, Yun Xiong, Xinyu Gao, Kangxiang Jia, Jinliu Pan, Yuxi Bi, Yi Dai, Jiawei Sun, and Haofen Wang, “Retrieval-augmented generation for large language models: A survey,” *arXiv preprint arXiv:2312.10997*, 2023.

[6] Guangzhi Xiong, Qiao Jin, Zhiyong Lu, and Aidong Zhang, “Benchmarking retrieval-augmented generation for medicine,” in *Findings of the Association for Computational Linguistics ACL 2024*, 2024, pp. 6233–6251.

[7] Peng Xia, Kangyu Zhu, Haoran Li, Tianze Wang, Weijia Shi, Sheng Wang, Linjun Zhang, James Zou, and Huaxiu Yao, “Mmed-rag: Versatile multimodal rag system for medical vision language models,” *arXiv preprint arXiv:2410.13085*, 2024.

[8] Hao Chen, Hongrun Zhang, U Wang Chan, Rui Yin, Xiaofei Wang, and Chao Li, “Domain game: Disentangle anatomical feature for single domain generalized segmentation,” in *International Workshop on Computational Mathematics Modeling in Cancer Analysis*. Springer Nature Switzerland Cham, 2024, pp. 41–51.

[9] Nengbo Wang, Xiaotian Han, Jagdip Singh, Jing Ma, and Vipin Chaudhary, “Causalrag: Integrating causal graphs into retrieval-augmented generation,” *arXiv preprint arXiv:2503.19878*, 2025.

[10] Weixing Chen, Yang Liu, Ce Wang, Jiarui Zhu, Guanbin Li, Cheng-Lin Liu, and Liang Lin, “Cross-modal causal representation learning for radiology report generation,” *IEEE Transactions on Image Processing*, 2025.

[11] Judea Pearl, *Causality: Models, Reasoning, and Inference*, Cambridge university press, 2009.

[12] Jing Ma, “Causal Inference with Large Language Model: A Survey,” Sept. 2024, arXiv:2409.09822 [cs].

[13] Yung-Sung Chuang, Yujia Xie, Hongyin Luo, Yoon Kim, James Glass, and Pengcheng He, “Dola: Decoding by contrasting layers improves factuality in large language models,” *arXiv preprint arXiv:2309.03883*, 2023.

[14] Qidong Huang, Xiaoyi Dong, Pan Zhang, Bin Wang, Conghui He, Jiaqi Wang, Dahua Lin, Weiming Zhang, and Nenghai Yu, “Opera: Alleviating hallucination in multi-modal large language models via over-trust penalty and retrospection-allocation,” *arXiv preprint arXiv:2311.17911*, 2023.

[15] Sicong Leng, Hang Zhang, Guanzheng Chen, Xin Li, Shijian Lu, Chunyan Miao, and Lidong Bing, “Mitigating object hallucinations in large vision-language models through visual contrastive decoding,” *arXiv preprint arXiv:2311.16922*, 2023.

[16] Sunan He, Yuxiang Nie, Zhixuan Chen, Zhiyuan Cai, Hongmei Wang, Shu Yang, and Hao Chen, “Meddr: Diagnosis-guided bootstrapping for large-scale medical vision-language learning,” *arXiv preprint arXiv:2404.15127*, 2024.

[17] Liwen Sun, James Zhao, Megan Han, and Chenyan Xiong, “Fact-aware multimodal retrieval augmentation for accurate medical radiology report generation,” *arXiv preprint arXiv:2407.15268*, 2024.

[18] Peng Xia, Kangyu Zhu, Haoran Li, Hongtu Zhu, Yun Li, Gang Li, Linjun Zhang, and Huaxiu Yao, “Rule: Reliable multimodal rag for factuality in medical vision language models,” *arXiv preprint arXiv:2407.05131*, 2024.

[19] Edward J Hu, Yelong Shen, Phillip Wallis, Zeyuan Allen-Zhu, Yuanzhi Li, Shean Wang, Lu Wang, and Weizhu Chen, “Lora: Low-rank adaptation of large language models,” *arXiv*, 2021.

[20] Omid Nejati Manzari, Hamid Ahmadabadi, Hossein Kashiani, Shahriar B Shokouhi, and Ahmad Ayatollahi, “Medvit: a robust vision transformer for generalized medical image classification,” *Computers in biology and medicine*, vol. 157, pp. 106791, 2023.

[21] Emily Alsentzer, John R Murphy, Willie Boag, Wei-Hung Weng, Di Jin, Tristan Naumann, and Matthew McDermott, “Publicly available clinical bert embeddings,” *arXiv preprint arXiv:1904.03323*, 2019.

- [22] Alistair EW Johnson et al., “Mimic-cxr: A large publicly available database of labeled chest radiographs,” *Scientific Data*, 2019.
- [23] Dina Demner-Fushman, Marc D Kohli, Marc B Rosenman, Sonya E Shooshan, Laritza Rodriguez, Sameer Antani, George R Thoma, and Clement J McDonald, “Preparing a collection of radiology examinations for distribution and retrieval,” *Journal of the American Medical Informatics Association*, vol. 23, no. 2, pp. 304–310, 2016.